The Geological Society of America
Field Guide 15
2009

The post-Mazama northwest rift zone eruption at Newberry Volcano, Oregon

Daniele Mckay*
Department of Geological Sciences, 1272 University of Oregon, Eugene, Oregon 97403-1272, USA

Julie M. Donnelly-Nolan*
U.S. Geological Survey, 345 Middlefield Road, Menlo Park, California 94025, USA

Robert A. Jensen*
U.S. Forest Service (retired), Bend, Oregon 97701, USA

Duane E. Champion*
U.S. Geological Survey, 345 Middlefield Road, Menlo Park, California 94025, USA

ABSTRACT

The northwest rift zone (NWRZ) eruption took place at Newberry Volcano ~7000 years ago after the volcano was mantled by tephra from the catastrophic eruption that destroyed Mount Mazama and produced the Crater Lake caldera. The NWRZ eruption produced multiple lava flows from a variety of vents including cinder cones, spatter vents, and fissures, possibly in more than one episode. Eruptive behaviors ranged from energetic Strombolian, which produced significant tephra plumes, to low-energy Hawaiian-style. This paper summarizes and in part reinterprets what is known about the eruption and presents information from new and ongoing studies. Total distance spanned by the eruption is 32 km north-south. The northernmost flow of the NWRZ blocked the Deschutes River upstream from the city of Bend, Oregon, and changed the course of the river. Renewed mafic activity in the region, particularly eruptions such as the NWRZ with tephra plumes and multiple lava flows from many vents, would have significant impacts for the residents of Bend and other central Oregon communities.

*dmckay1@uoregon.edu; jdnolan@usgs.gov; bjensen@bendnet.com; dchamp@usgs.gov

Mckay, D. Donnelly-Nolan, J.M., Jensen, R.A., and Champion, D.E., 2009, The post-Mazama northwest rift zone eruption at Newberry Volcano, Oregon, *in* O'Connor, J.E., Dorsey, R.J., and Madin, I.P., eds., Volcanoes to Vineyards: Geologic Field Trips through the Dynamic Landscape of the Pacific Northwest: Geological Society of America Field Guide 15, p. 91–110, doi: 10.1130/2009.fld015(05).

INTRODUCTION

The post-Mazama northwest rift zone eruption (NWRZ) of Newberry Volcano, Oregon, took place ~7000 years ago subsequent to the eruption that produced the Crater Lake caldera ~7650 years ago (Hallett et al., 1997) and mantled Newberry with Mazama ash. The NWRZ includes multiple lava flows from a variety of vents along northwest trends over a north-south distance of ~32 km (Fig. 1). Lavas ranging in composition from basalt through andesite erupted from cinder cones and spatter vents extending from the low northwest flank of the volcano to the inner north wall of the caldera, and south to include one eruption on the upper southwest flank. This eruptive event represents the most recent mafic volcanic activity at Newberry, which is dotted with some 400 mafic cinder cones and fissure vents (MacLeod and Sherrod, 1988).

The mafic lava flows of the NWRZ were described briefly by Nichols and Stearns (1938), who wrote that the fissure eruption extended from north of Lava Butte to the fissure described by Williams (1935) on the north wall of the caldera. Peterson and Groh (1965) first used the term "Northwest Rift Zone." Characteristics of the eruption that support the use of the term "rift zone" include multiple parallel fissures and aligned vents, as well as fractures. Peterson and Groh (1965) published the first map of the lava flows and named many of them. MacLeod et al. (1995) divided the "Young basaltic andesite" of the northwest rift zone into 15 lava flows (Qyb 1–15) and a separate unit for vents (Qyc). They included five lava flows (Qyb 10, 11,13–15) not identified by Peterson and Groh (1965), most notably the Surveyors flow on the upper southwest flank of the volcano.

In this paper we summarize and discuss the previous work on the NWRZ, suggest revised interpretations, and present the results of new and ongoing work. Potential hazards of a similar eruption in the future are addressed, and possible future avenues of research are outlined.

THE NORTHWEST RIFT ZONE (NWRZ) ERUPTION

The NWRZ flows are mostly treeless and very youthful in appearance, ranging in morphology from fluid pahoehoe to 'a'a and block lava. New geologic work indicates that some previously included lava flows are not part of the NWRZ, which is here reinterpreted to include twelve informally named lava flows, one very small unnamed flow, and the East Lake Fissure (Fig. 2). We conclude that two flows included by MacLeod et al. (1995) were not part of the eruption. One of these is The Dome and its lava flows, which are mantled by Mazama ash. We also exclude the Devils Horn flow, which was included in the NWRZ by MacLeod et al. (1995) although they recognized that it predates the Mazama ash bed.

The flow and vent types are listed in Table 1 along with areas, volumes, and vent elevations. Total area covered by the lava flows is ~68 km^2; total estimated erupted volume including tephra is ~0.86 km^3. Elevations of vents range from ~1375 m to ~2230 m. Over 90% of the NWRZ volume was erupted below 1750 m elevation, and in the northwesternmost 11 km of the rift zone (north group of Table 1). The only two large cinder cones, Lava Butte and Mokst Butte, were erupted in this northwestern portion of the rift. These two cones produced the two largest lava flows that together account for 80% of the total eruptive volume. The northernmost flow, the Lava Butte flow, is one of the most voluminous at over 0.3 km^3. This is the lava flow that temporarily blocked the Deschutes River and changed the river's course.

With a single exception, all vents in the southern portion (south group of Table 1 and Fig. 2) of the rift are spatter vents. Only the central vent in the spatter rampart of the Surveyors flow at the far southern end of the NWRZ can be considered as a small cinder cone. Spatter vents are also features of the northwestern section of the rift zone, although they produced only very small volume lava flows (North Sugarpine and Gas-Line).

The northwestern portion (north group of Table 1 and Fig. 2) of the NWRZ is also the widest, spanning multiple fissures across 10 km from the North Sugarpine and South Sugarpine vents to the Mokst flow vents and still farther east to the South Kelsey vents. Southeast of these vents, in the south group, the vent locations are narrowly focused, with the NWRZ not exceeding 1 km in width from the Forest Road flow to the East Lake Fissure. From there, the eruption stepped south 10 km and slightly to the west to the Surveyors flow vents. No stratigraphic relationship exists to indicate the age of the north group relative to the south group.

Paleomagnetic and Radiocarbon Data

Samples for paleomagnetic study were collected in 1974 and 1976. Cores were drilled from outcrops using a handheld, gasoline-powered 1-inch diameter coring drill. The East Lake Fissure and ten of the lava flows were sampled, in some cases from multiple sites within a single flow. Core samples from all sites were oriented using a sun compass, measured in the U.S. Geological Survey laboratory in Menlo Park, California, using a spinner magnetometer, and representative samples were tested by alternating-field (AF) demagnetization. Most sites were found to have no secondary magnetic components and were not demagnetized, while 4 sites were given blanket AF demagnetization of 20 or 30 mT. Characteristic remanent magnetization for each site was calculated using Fisherian statistics, and are listed in Table 2, and plotted in Figure 3. Results for the individual sites were originally published in Champion (1980) and published again in Hagstrum and Champion (2002), although we reinterpret the overall results.

In Table 2 and on Figure 3, we present a mean direction for 11 of the 12 sites. The average direction has a 95% confidence circle of 1.9° radius, representing a well-grouped distribution. For this calculation, we excluded the site taken on the Mokst flow. The direction obtained for that site is noticeably different and does not overlap any of the other measured directions. The Mokst flow is an extremely rugged 'a'a and block lava flow that offers rare options for drilling in-place lava that has not been rotated since it was emplaced.

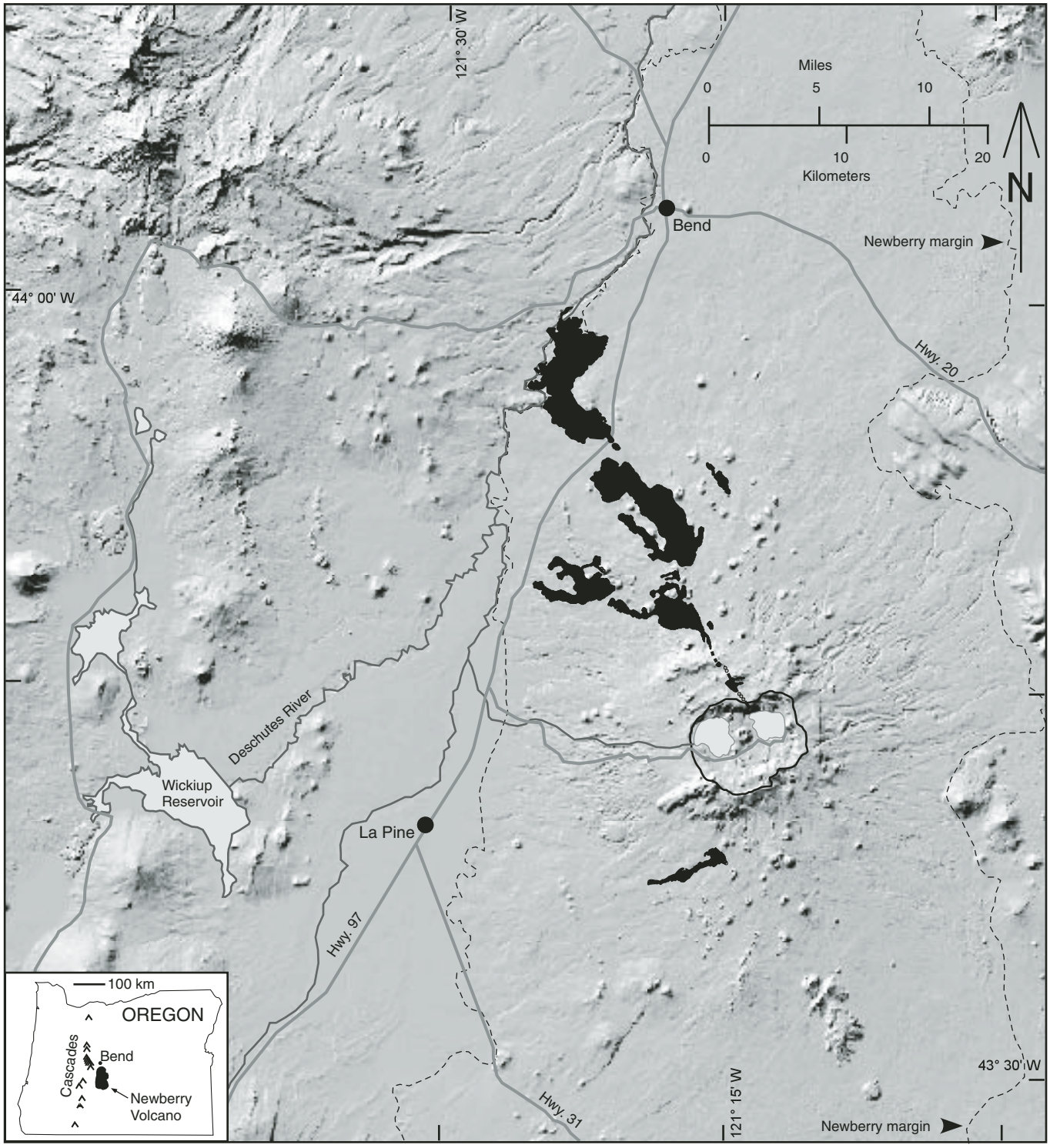

Figure 1. Shaded relief regional location map showing Newberry Volcano (outline marked by dashed line) with northwest rift zone lavas shown in black. Numerous cinder cones are visible on the flanks of the Newberry edifice and to the west toward the Cascade crest.

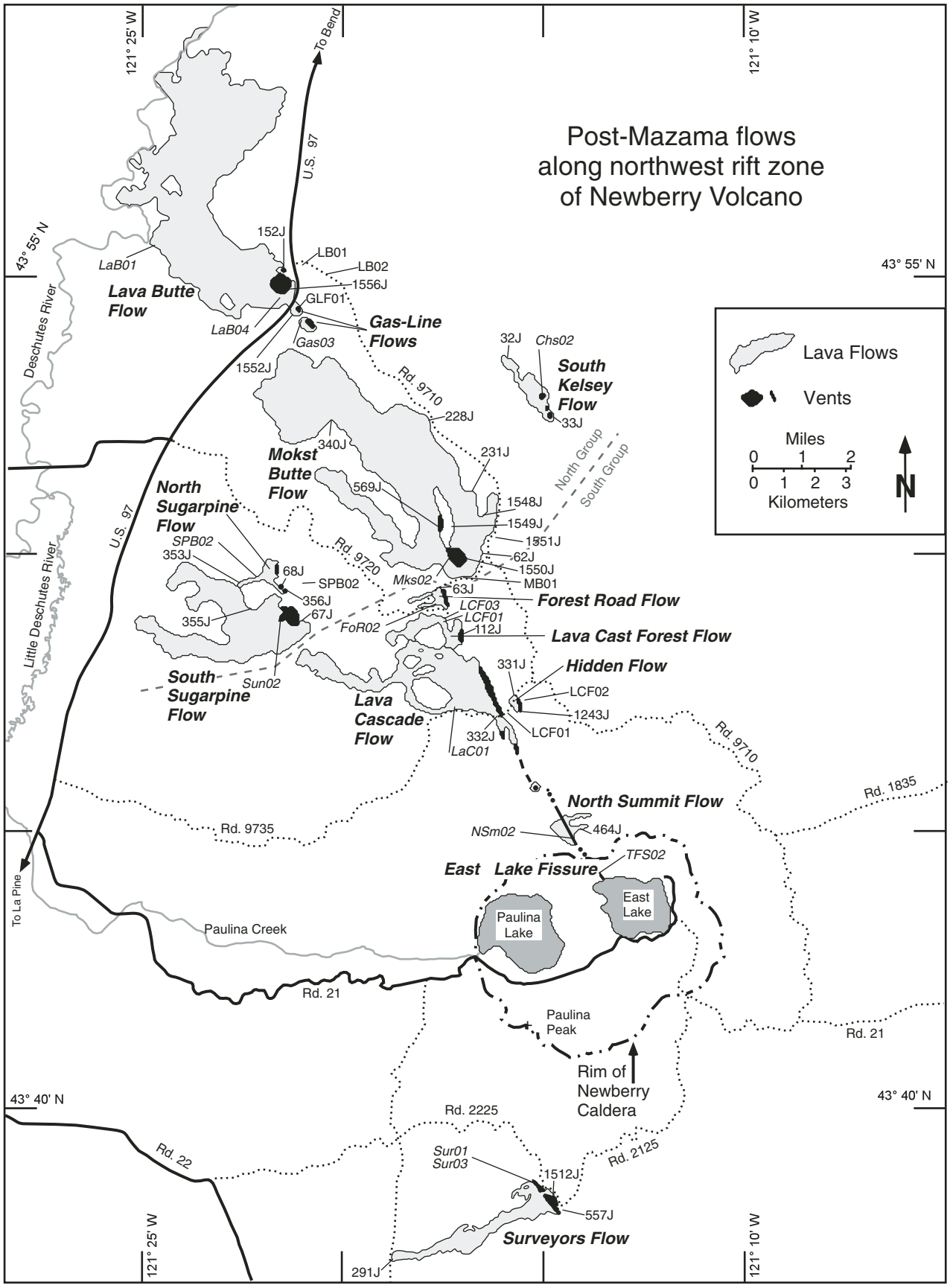

Figure 2. Map shows location and distribution of northwest rift zone lavas and vents, their names (informal), and the locations of analyzed samples. Paved roads are shown with solid lines; major graveled roads shown with dotted lines. North and south groups are indicated.

TABLE 1. NORTHWEST RIFT ZONE (NWRZ) PARAMETERS

Unit	Vent type	Vent elevation (m)	Flow type	Average flow thickness (m)	Area of flow (km^2)	Eruptive volumes (10^6 m^3)				% of total NWRZ eruption	% of total unit volume		
						Flow	Vent (DRE)	Tephra (DRE)	Total		Flow	Vent	Tephra
North Group													
Lava Butte	Large cone	1375	‘a‘a	12	23.52	282.0	24.6	2.6	309.2	35.9	91.2	8.0	0.8
Gas-Line	Spatter	1375	phh	3	0.34	1.0	0.1	0.03	1.1	0.1	88.5	8.9	2.6
Mokst Butte	Large cone	1725	‘a‘a block	15	23.96	359.4	20.4	2.1	381.9	44.3	94.1	5.3	0.6
South Kelsey	Small cones	1550	‘a‘a phh	9	1.19	10.7	0.5	?	11.2	1.3	95.5	4.5	0.0
North Sugarpine	Spatter	1465	phh	2	0.52	1.0	0.02	?	1.0	0.1	98.0	2.0	0.0
South Sugarpine	Small cone	1500	‘a‘a phh	12	7.74	92.9	7.6	1.1	101.6	11.8	91.4	7.5	1.1
North Group Totals					57.27	747.0	53.2	5.8	806.0	93.5	92.7	6.6	0.7
South Group													
Forest Road	Spatter	1750	phh ‘a‘a	3	0.41	1.2	0.02	0.003	1.2	0.1	98.1	1.6	0.3
Lava Cast Forest	Spatter	1770	phh ‘a‘a	3	1.32	4.0	0.1	0.2	4.3	0.5	93.0	2.3	4.7
Lava Cascade	Spatter	1830	phh ‘a‘a	5	6.92	34.6	2.5	1.6	38.7	4.5	89.4	6.5	4.1
Hidden	Spatter	1880	phh ‘a‘a	2	0.18	0.4	0.03	0.002	0.4	0.1	92.6	6.9	0.5
Unnamed	Spatter	2140	phh ‘a‘a	1	0.05	0.1	0.02	?	0.1	0.0	83.3	16.7	0.0
North Summit	Spatter	2230	phh ‘a‘a	3	0.26	0.8	0.06	?	0.9	0.1	93.0	7.0	0.0
East Lake Fissure	Spatter	2130	none	0	0.00	0.0	0.2	?	0.2	0.0	0.0	100.0	0.0
Surveyors	Spatter+ small cone	1770	‘a‘a phh	3	2.90	8.7	0.8	0.9	10.4	1.2	83.6	7.7	8.7
South Group Totals					12.04	49.8	3.7	2.7	56.2	6.5	88.6	6.6	4.8
NWRZ Totals					69	797	57	8	862	100 %	92	7	1

Note: Flow areas were measured in a CAD program, while flow thicknesses are estimates of average thickness. Thus flow and total volumes are best estimates. NWRZ totals given to nearest whole number. DRE—dense rock equivalent, calculated using values in McKnight and Williams (1997); phh—pahoehoe.

TABLE 2. NORTHWEST RIFT ZONE PALEOMAGNETIC DATA

Lava flows	Site	Lat.	Long.	N/No	Exp.	I	D	α95	k	R	Plat.	Plong.
North Group												
Lava Butte	LaBO	43.914°	238.642°	22/25	NRM	58.4°	351.5°	2.0°	245	21.91434	82.0°	114.1°
Gas-Line	GasO	43.907°	238.654°	12/12	NRM	57.6°	343.1°	2.3°	367	11.97003	76.1°	130.5°
Mokst Butte	MksO	43.834°	238.713°	10/12	30	(65.3°	343.0°)	3.5°	193	9.95334	77.6°	171.2°
South Kelsey	ChsO	43.883°	238.752°	11/13	20+	59.7°	350.3°	2.2°	420	10.97620	82.1°	126.9°
North Sugarpine	SPBO	43.828°	238.636°	12/12	30	58.2°	353.7°	4.4°	98	11.88768	83.2°	104.5°
South Sugarpine	SunO	43.818°	238.650°	12/12	20	57.7°	355.1°	2.8°	238	11.95374	83.4°	94.7°
		43.85°	238.7°	5/6		58.4°	350.7°	2.5°	967	4.99586	81.6°	117.4°
South Group												
Forest Road	ForO	43.820°	238.709°	20/20	NRM	51.8°	353.9°	1.4°	574	19.96689	77.7°	83.4°
Lava Cast Forest	LCFO	43.816°	238.711°	21/24	NRM	52.5°	352.9°	2.3°	188	20.89365	77.9°	88.4°
Lava Cascade	LaCO	43.788°	238.715°	24/24	NRM	55.3°	352.6°	3.6°	69	23.66515	80.2°	96.8°
North Summit	NSmO	43.750°	238.766°	13/15	NRM	54.9°	355.3°	3.8°	119	12.89950	81.0°	83.9°
East Lake Fissure	TFsO	43.736°	238.777°	12/12	NRM	57.0°	358.6°	2.3°	356	11.96908	83.8°	68.9°
Surveyors	SurO	43.643°	238.747°	24/24	NRM	53.3°	354.1°	2.3°	169	23.86371	79.2°	85.8°
		43.75°	238.75°	6/6		54.2°	354.5°	1.9°	1223	5.99591	80.0°	85.7°
All Sites		43.8°	238.7°	11/12		56.1°	352.9°	1.9°	571	10.98250	81.0°	98.2°

Note: Site is alphabetic site label. Lat./Long. are site latitude(°N) and longitude(°E) in degrees. N/No is the number of cores used in site averaging compared to the number of independent cores taken. Exp. is the peak alternating-field strength used in blanket demagnetization, (NRM) indicated that no demagnetization was necessary. I and D are remanent inclination and declination of site mean direction in degrees. α95 is the 95% confidence limit about the mean direction. k is the estimate of the Fisherian precision parameter. R is the length of the resultant vector. Plat./Plong. is the location in °N and °E of the virtual geomagnetic pole (VGP) calculated from the site mean direction. Parentheses around the Mokst Butte site mean direction indicate it was not used in group mean.

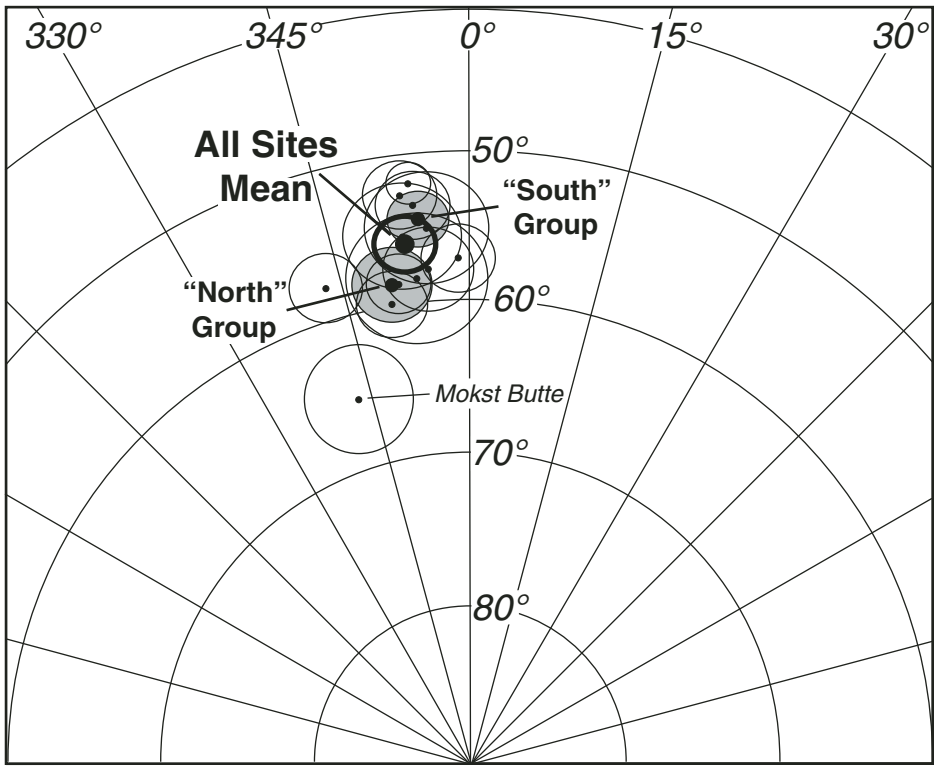

Figure 3. Portion of lower hemisphere equal-area diagram showing mean directions of remanent magnetization recorded in lava from 12 vents of the northwest rift zone (small black dots). Each direction is surrounded by circle of 95% confidence. Mean direction for 11 of 12 sites, excluding Mokst Butte (see discussion in text), is shown with largest black dot and bold 95% confidence circle. Shaded circles are confidence limits surrounding mean directions (mid size black dots) for north and south groups of vents, (see Table 2). Mokst Butte is located in the north group, but it was not included in the north group mean direction.

The results show that there is little range in average remanent directions for these sites, and much overlap, supporting the idea that these post-Mazama flows represent a short eruptive event. However, careful examination of the remanent inclination values (Table 2) indicates that flows in the north group have systematically steeper inclination values than flows in the south group (Fig. 3). Separate mean directions of magnetization calculated for the north and south groups (Table 2; Fig. 3) show them to be distinct and separable remanent magnetic populations, not recording the same remanent direction. The 4° angular separation in recorded magnetic direction could require many decades to possibly a century of time to have elapsed between the times of eruption of the north and south groups of vents (Champion and Shoemaker, 1977).

Multiple radiocarbon dates have been performed on samples collected from the NWRZ. MacLeod et al. (1995) include a table listing 11 radiocarbon dates for this eruption, with samples obtained from 8 different flows as reported by 5 different sources published from 1969 to 1990. The calibrated calendar ages range from 6610 to 7240 yr B.P. The average of all the ages listed in MacLeod et al. (1995) is 6927 yr B.P. and thus we use 7000 years ago as an estimate of the eruption age. Sub-averages of the radiocarbon ages for the north group of NWRZ lavas and the south group are nearly identical to each other. Thus, the possible time gap indicated by paleomagnetic data is not reflected in the radiocarbon data. The span of more than 600 years indicated by the range of measured ages suggests that the resolution of the existing radiocarbon data is inadequate to identify a time interval between episodes of eruptive activity along the NWRZ. Factors such as the type and location of a sample within the original burned tree, and the quality and thoroughness of radiocarbon sample pretreatment likely contribute to the span of measured ages and cannot be known from the existing data.

Erupted Compositions

Lava compositions listed in Table 3 and shown in Figure 4 range from basalt (51.3 wt% SiO_2) to andesite (58.4 wt% SiO_2), but are dominantly in the basaltic andesite range (between 52.1 and 56.9 wt% SiO_2). Compositional variation of the NWRZ was previously documented by MacLeod et al. (1995, map explanation), who presented silica contents of many of the lava flows. A handful of complete analyses of NWRZ lavas are given in MacLeod and Sherrod (1988).

Vent type and SiO_2 content do not appear to be correlated in this eruption. The lowest-SiO_2 vents are spatter vents and produced fluid pahoehoe lava flows at North Sugarpine. However, among the highest-SiO_2 vents, Mokst Butte at 57.4% SiO_2 built a large cinder cone, whereas farther south spatter vents have even higher SiO_2 contents. The Lava Cascade spatter vents have 57.5% SiO_2, and a spatter vent for the Hidden flow has even higher SiO_2 at 57.8%. A sample of the East Lake Fissure, which consists entirely of spatter, also has high silica with 57.3%. However, these southern vents produced much smaller volumes of lava. One possible explanation for the drastic difference in vent morphology at the same high silica content could be that the southern spatter vents were only in eruption for a very short period, never building into large cones. Another possible explanation might be that the andesitic magma was unusually hot, and thus more fluid than typical andesite lavas. By contrast, Mokst Butte lava may have been more volatile-rich.

Variation diagrams (Fig. 4) demonstrate the wide compositional range of the NWRZ lavas. However, all analyzed samples fall into the calc-alkaline field. The plots in Figure 4 show that the northwestern lavas (north group of Table 1 and Fig. 2) display a wider range of compositions than the much less voluminous south group lavas. North and south group andesites show considerable overlap. Andesite (lava with 57%–62% SiO_2) is a relatively rare composition at Newberry.

Strontium contents of NWRZ lavas with <4.7 wt% MgO range from 280 to 361 ppm (Fig. 4, Table 3). By contrast the two flows that were included in the NWRZ by MacLeod et al. (1995), but excluded by us have Sr contents at approximately the same MgO content (<4.6 wt%) of 497–502 ppm (The Dome) and 582–649 ppm (Devils Horn). Thus, besides their stratigraphic position below the Mazama ash bed, the significantly higher Sr values distinguish these two flows from the NWRZ.

Petrographically, only the North and South Sugarpine flows display noticeable amounts of phenocrysts. They contain 1%–2% of phenocrysts, dominantly 1 mm plagioclase, but occasionally 2 mm plagioclase and 1 mm olivine, and rarely 1 mm clinopyroxene. In addition, however, 1–2 cm crystal clots containing plagioclase+olivine+clinopyroxene are common. These clots are rarely seen in the other flows of the NWRZ, which typically contain less (and commonly much less) than 1% of phenocrysts, nearly always plagioclase, but occasionally including olivine.

It is apparent on Figure 4 that the Hidden flow lavas of the south group and the Mokst flow lavas of the north group have similar compositions. They are also located on the same northwest trend, slightly offset from the northwest trend that includes the Lava Butte, Lava Cast Forest, Lava Cascade, etc., flows. No study has been done, however, to assess the petrologic relationships among the lavas.

VENTS AND TEPHRAS OF THE NWRZ

In addition to the mapped lava flows, isopachs of tephra deposits produced by several of the vents were also mapped (MacLeod et al., 1995). More than 400 holes were dug or augered between 1977 and 1986 to determine the thickness and shape of the tephra plumes related to 9 vents along the NWRZ. Depths were readily determined in most holes over a third of a meter deep because of the easily identified underlying Mazama ash bed. In shallower holes, root throw and animal burrows have thoroughly obscured the contact and the trace limit was visually established based on lack of surficial tephra fragments.

The eruption produced examples of the types of mafic vents that are abundant on the flanks of Newberry Volcano, including

TABLE 3. CHEMICAL ANALYSES OF NORTHWEST RIFT ZONE LAVA AND VENT SAMPLES

No.:	Lava Butte				Gas-Line		Mokst Butte								South Kelsey			North Sugarpine			
	LaB 01	152 J	1556 J	LaB 04	1552 J	Gas 03	228 J	340 J	231 J	1548 J	569 J	1550 J	Mks 02	62 J	33 J	32 J	Chs 02	SPB 02	353 J	68 J	356 J
wt%																					
SiO_2	55.3	56.1	56.2	56.1	55.4	55.4	57.5	58.4	57.6	57.2	57.8	57.4	57.2	58.0	55.6	55.6	55.6	51.7	51.9	51.8	51.8
Al_2O_3	17.3	17.2	17.2	17.1	17.3	17.3	15.9	15.8	15.8	16.0	15.9	16.1	16.0	15.9	16.5	16.5	16.5	17.3	17.4	17.3	17.4
FeO*	7.43	7.11	7.04	7.08	7.23	7.18	7.81	7.47	7.74	7.81	7.60	7.71	7.86	7.60	8.21	8.24	8.21	8.68	8.63	8.69	8.60
MgO	5.10	5.00	4.91	5.04	5.27	5.31	4.16	4.09	4.26	4.37	4.31	4.15	4.31	4.09	4.72	4.65	4.69	6.31	6.32	6.32	6.34
CaO	8.10	8.00	7.99	7.99	8.37	8.27	7.32	6.88	7.26	7.44	7.14	7.26	7.28	6.96	7.87	7.90	7.86	9.95	9.92	9.98	9.97
Na_2O	3.94	3.72	3.88	3.85	3.73	3.77	3.98	3.98	4.01	3.94	3.94	4.06	3.98	4.00	3.96	3.94	4.00	3.55	3.36	3.46	3.47
K_2O	1.23	1.35	1.35	1.33	1.25	1.25	1.64	1.78	1.68	1.63	1.70	1.65	1.66	1.75	1.33	1.35	1.34	0.67	0.63	0.66	0.64
TiO_2	1.17	1.08	1.06	1.09	1.09	1.08	1.26	1.23	1.26	1.28	1.22	1.28	1.28	1.24	1.35	1.35	1.34	1.34	1.35	1.33	1.35
P_2O_5	0.29	0.26	0.22	0.27	0.23	0.26	0.28	0.27	0.28	0.21	0.22	0.22	0.26	0.26	0.29	0.30	0.28	0.31	0.32	0.31	0.32
MnO	0.14	0.13	0.13	0.13	0.14	0.13	0.14	0.14	0.14	0.15	0.14	0.15	0.15	0.14	0.15	0.15	0.15	0.16	0.16	0.15	0.15
ppm																					
Rb	27	31	32	29	29	26	46	49	47	43	46	43	39	44	29	29	30	8	11	17	11
Sr	410	359	387	390	400	389	291	280	289	298	288	293	307	280	330	335	325	435	433	435	432
Y	26	24	25	25	24	24	32	33	31	31	31	32	30	31	30	29	25	22	23	27	25
Zr	169	154	156	167	143	146	172	188	173	169	180	180	191	191	180	181	180	113	114	116	115
Nb	15	12	9	13	10	12	12	14	13	12	13	11	14	16	13	15	17	11	10	11	11
Ba	342	351	370	351	335	364	426	418	435	388	394	400	376	398	348	349	369	229	219	232	222
Ni	40	39	47	47	52	53	25	19	23	20	23	17	28	25	29	23	31	44	44	37	42
Cu	63	74	67	73	62	79	60	57	49	59	58	54	66	60	61	56	63	85	88	84	93
Zn	75	80	73	80	72	71	73	77	74	81	76	76	75	81	80	75	84	79	76	72	76
Cr			102		114		35	37	37	47	43	43							129		132
Ce			31		27		32	36	38	34	34	35							22		21
Ga			18		18		20	18	18	18	20	18							21		17
La			16		16		15	16	20	16	14	15							12		8
Nd			16		17		23	15	16	18	21	19							17		18
V			167		176		198	183	196	198	179	194							221		226
N 43°	55.75	55.32	55.00	54.85	54.54	54.42	52.48	52.43	51.24	50.86	50.47	50.23	50.07	50.05	52.65	53.66	52.97	49.67	49.63	49.52	49.43
W 121°	24.46	21.38	21.12	21.48	21.06	20.77	17.60	20.19	16.50	16.17	17.20	16.67	17.25	16.33	14.40	15.67	14.89	21.87	22.36	21.40	21.24

Note: Sample locations are shown on Fig. 2. Chemical analyses performed at U.S. Geological Survey, Denver, Colorado, except 1512J, 1548J, 1550J, 1552J, and 1556J, which were analyzed at Washington State University. Major element analyses are normalized to 100% volatile-free with all iron calculated as FeO and indicated as FeO*. Latitude/Longitude locations are all in decimal minutes. ELF—East Lake Fissure.

(*continued*)

TABLE 3. CHEMICAL ANALYSES OF NORTHWEST RIFT ZONE LAVA AND VENT SAMPLES (*continued*)

	South Sugarpine			Forest Road		Lava Cast Forest			Lava Cascade		Hidden		North Summit		ELF	Surveyors			
No.:	355 J	Sun 02	67 J	63 J	FoR 02	LCF 03	LCF 01	112 J	LaC 01	332 J	331 J	1243 J	464 J	NSm 02	TFS 02	Sur 01	Sur 03	1512 J	291 J
wt%																			
SiO_2	53.4	52.1	53.2	53.7	53.6	54.2	54.1	53.5	54.9	57.5	57.8	57.7	55.2	55.3	57.3	55.1	55.8	56.7	55.3
Al_2O_3	16.7	17.1	16.9	17.3	17.3	17.1	17.1	17.4	16.9	16.4	15.8	15.6	16.8	16.9	16.5	16.9	16.8	16.9	16.9
FeO*	8.73	8.68	8.61	8.19	8.15	8.03	8.07	8.22	7.96	7.53	7.68	7.83	7.94	7.92	7.55	7.69	7.49	7.23	7.67
MgO	5.36	6.09	5.59	5.47	5.58	5.32	5.41	5.59	5.03	3.99	4.31	4.25	4.89	4.78	3.98	5.23	4.98	4.57	5.22
CaO	9.14	9.80	9.28	9.03	9.10	8.81	8.89	9.14	8.44	7.14	7.21	7.28	8.37	8.27	7.20	8.40	8.08	7.68	8.36
Na_2O	3.73	3.65	3.66	3.65	3.72	3.82	3.74	3.65	3.94	4.12	3.90	4.15	3.90	3.94	4.17	3.83	3.93	3.96	3.68
K_2O	0.90	0.72	0.88	0.92	0.87	1.03	0.92	0.87	1.13	1.51	1.66	1.67	1.12	1.17	1.56	1.15	1.29	1.43	1.21
TiO_2	1.46	1.36	1.37	1.27	1.27	1.27	1.26	1.28	1.26	1.28	1.25	1.24	1.28	1.27	1.29	1.23	1.20	1.18	1.21
P_2O_5	0.34	0.31	0.34	0.32	0.30	0.30	0.30	0.27	0.31	0.33	0.25	0.21	0.32	0.31	0.31	0.31	0.30	0.27	0.33
MnO	0.16	0.16	0.16	0.15	0.15	0.15	0.15	0.15	0.15	0.14	0.14	0.15	0.15	0.15	0.14	0.15	0.14	0.14	0.14
ppm																			
Rb	19	16	19	23	24	21	19	15	23	38	45	45	25	25	36	26	32	36	29
Sr	403	416	384	419	446	434	405	409	410	361	288	299	393	391	338	394	360	359	383
Y	27	23	23	24	24	23	24	28	23	37	32	32	31	27	28	25	26	29	28
Zr	141	119	131	132	130	139	133	123	153	183	179	180	150	153	173	159	161	172	157
Nb	12	10	12	13	13	13	15	10	13	13	13	14	12	14	13	17	12	11	12
Ba	283	255	276	283	283	326	303	279	342	429	400	409	314	359	413	347	367	395	341
Ni	26	35	30	38	46	38	42	39	38	22	23		32	36	16	36	35	33	36
Cu	76	81	94	74	84	79	79	94	84	51	56	58	67	75	63	76	69	60	67
Zn	80	78	91	77	84	76	84	87	86	76	78	75	78	88	93	86	77	78	76
Cr	77									51	35	46	85					97	95
Ce	30									31	34		28					35	35
Ga	20									18	20	18	18					17	17
La	12									17	15		10					18	17
Nd	22									26	27		17					21	31
V	228									185	196	188	203					167	184
N 43°	49.15	49.06	49.02	49.40	49.19	48.97	48.94	48.64	47.30	47.16	47.45	47.07	45.07	44.99	44.15	38.60	38.60	38.32	37.20
W 121°	22.08	21.02	20.77	17.61	17.48	17.32	17.33	16.91	17.20	15.98	15.43	15.35	13.97	13.90	13.41	15.16	15.16	14.70	18.67

Note: Sample locations are shown on Fig. 2. Chemical analyses performed at U.S. Geological Survey, Denver, Colorado, except 1512J, 1548J, 1550J, 1552J, and 1556J, which were analyzed at Washington State University. Major element analyses are normalized to 100% volatile-free with all iron calculated as FeO and indicated as FeO*. Latitude/Longitude locations are all in decimal minutes. ELF—East Lake Fissure.

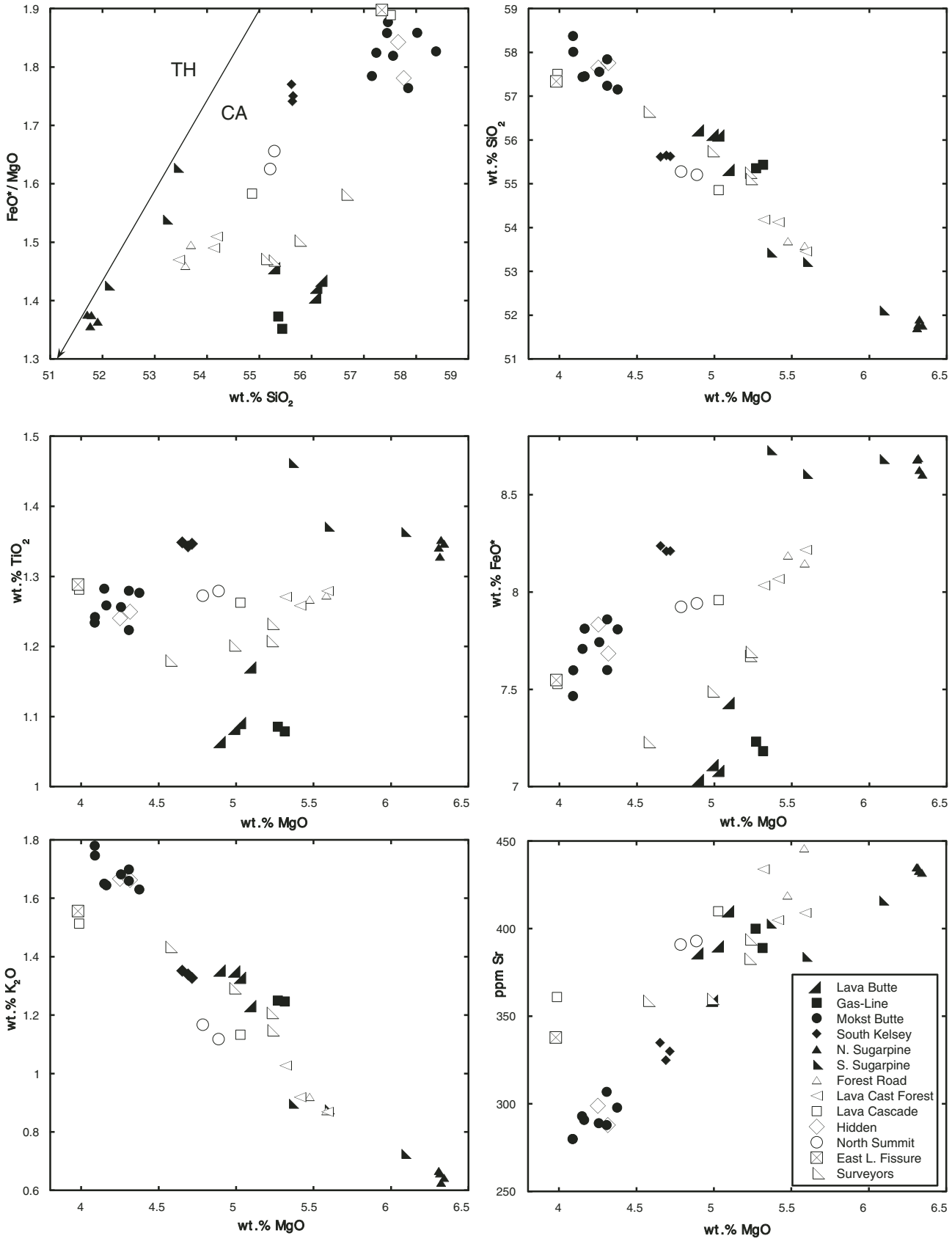

Figure 4. Variation diagrams showing chemical variability of northwest rift zone lavas (see Table 1). Tholeiitic (TH) and calc-alkaline (CA) dividing line from Miyashiro (1974).

large and small cinder cones, spatter cones and spatter ramparts, as well as fissures, representing both Strombolian and Hawaiian types of activity. It provides the opportunity to study a variety of eruption styles as they manifested in an eruptive event that took place over a relatively short interval of time.

Preliminary results from study of the NWRZ tephra and vent deposits are presented here. The variety of vent types and volumes of erupted materials make the NWRZ an interesting study area for the categorization of mafic eruptions. Some vent areas produced a variety of morphologies in a very small area, such as the 2.4 km fissure segment that produced the large Lava Butte cinder cone, an adjacent small cinder cone, and the spatter cones of the Gas-Line flows (Fig. 5). The Lava Butte vent also produced extensive lava flows and a tephra blanket. Other vents, such as the Lava Cascade vents, produced spatter cones, lava flows, and a tephra blanket, but no cinder cones. Physical differences in cone morphologies and differences in the tephra deposited from these two vents can be used to interpret differences in eruption styles.

Lava Butte Vents

The Lava Butte eruption began as a fissure eruption that produced the spatter cones and lavas of the Gas-Line flows. Eventually the eruption was focused into a single vent, which produced the Lava Butte cone, tephra blanket, and lava flows. The Lava Butte cinder cone reached a final height of ~150 m, a base diameter of ~700 m, and a crater depth of ~50 m. Prevailing winds from the southwest built the northeast rim of the cone ~25 m higher than the southwest rim. The cone appears to be constructed of loose scoria at the angle of repose, but internal construction is not exposed except at the rim and in the crater, where there are outcrops of moderately welded agglutinate. The tephra blanket was deposited to the northeast and covers an area of ~8 km^2. The proximal deposit is >5 m thick (Jensen, 2006). Trace deposits extend ~2.5 km from the vent, but presumably the original trace deposits extended much farther (e.g., Hill et al., 1998). The total estimated volume of the tephra deposit is ~2.6×10^6 m^3 dense rock equivalent (Table 1), which is probably a minimum. Lava emerged from the base of the cone at a bocca on the south side and multiple lobes merged and flowed northwest into the Deschutes River channel. The lava flowed ~11 km from the vent and covers an area of ~24 km^2.

Samples of the Lava Butte tephra were collected from pit LB01 ~300 m northeast of the cone (Fig. 6A). The sample pit was 2.5 m deep and did not reach the base of the deposit, although the base of the deposit was probably close based on comparison with the base of the deposit where it was reached at other locations. At location LB01, the deposit is made up of alternating layers of fine ash and fine to coarse lapilli (Fig. 7). The deposit was separated into four main sections (see stratigraphic horizons labeled A–D in Fig. 7) based on sharp contacts between massive lapilli layers and distinctive fine ash layers. Each stratigraphic horizon was

Figure 5. Photo from Gas-Line flow with spatter rampart visible on right, looking northwest toward the Lava Butte cinder cone (photo by R.A. Jensen). See also Jensen et al. (2009, this volume) for another photo of Lava Butte.

further subdivided and sampled based on changes between fine ash and fine to coarse lapilli. Individual layers within the deposit are well sorted (Fig. 7). The tephra is made up of three juvenile components that differ in vesicularity: (1) tan, highly vesicular scoria (sideromelane), (2) black, less vesicular scoria (tachylite), and (3) dense fragmented lava (Fig. 8). Sideromelane and tachylite clasts are similar to those observed at Cinder Cone, California (Heiken, 1978). All three components are crystal poor, as is the lava flow, but some clasts contain plagioclase phenocrysts. Loose crystals in the tephra are very rare. With regard to grain size, black scoria dominates in the <8 mm size range, whereas tan scoria dominates in the >8 mm size range (Fig. 9). The deposit

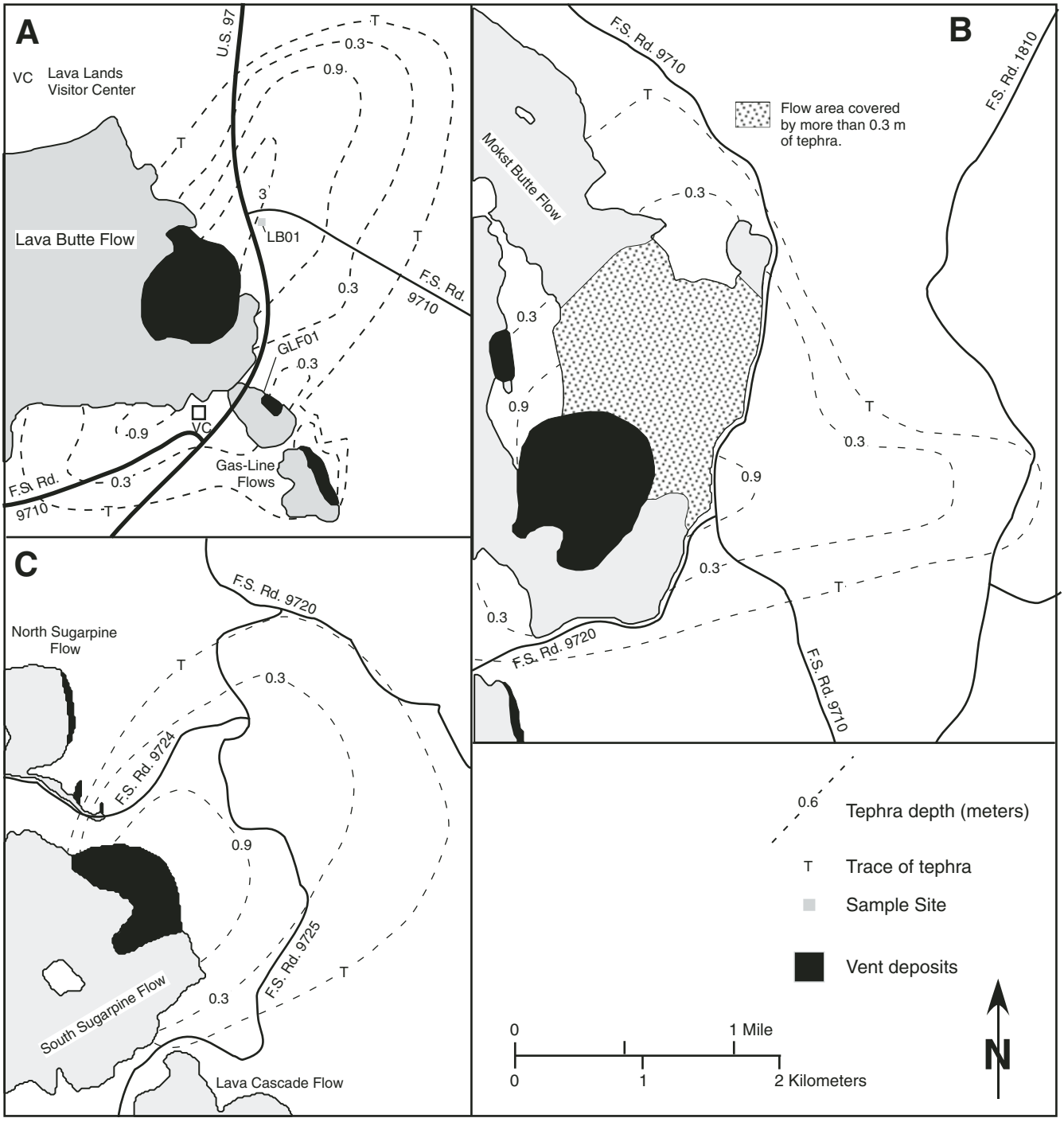

Figure 6 (*continued on next page*). (A–E) Maps showing isopachs of mapped tephra deposits (adapted from Jensen, 2006) and locations of tephra sample pits discussed in text.

also contains lapilli pyroclasts that resemble tan scoria but have flattened shapes with relatively smooth wavy surfaces (Fig. 8). Similar clasts (Fig. 10) have been observed in the tephra deposit from Paricutin, Mexico (Pioli et al., 2008).

Tephra from the Gas-Line vents is exposed in a quarry ~100 m east of U.S. Highway 97. This deposit differs from the Lava Butte tephra in covering significantly less area (Fig. 6A) and consisting of only one component, tan highly vesicular scoria. The tephra blanket is characterized by massive lapilli layers containing large, very vesicular, glassy clasts (Fig. 11). These large glassy clasts are common in the Gas-Line tephra but not seen in the Lava Butte tephra.

Lava Cascade Vents

The Lava Cascade vents are a series of northwest trending fissure vents that extend for ~3.5 km (Fig. 6D). Unlike the Lava Butte eruption, the Lava Cascade eruption did not become focused into a single vent and no cinder cone was formed.

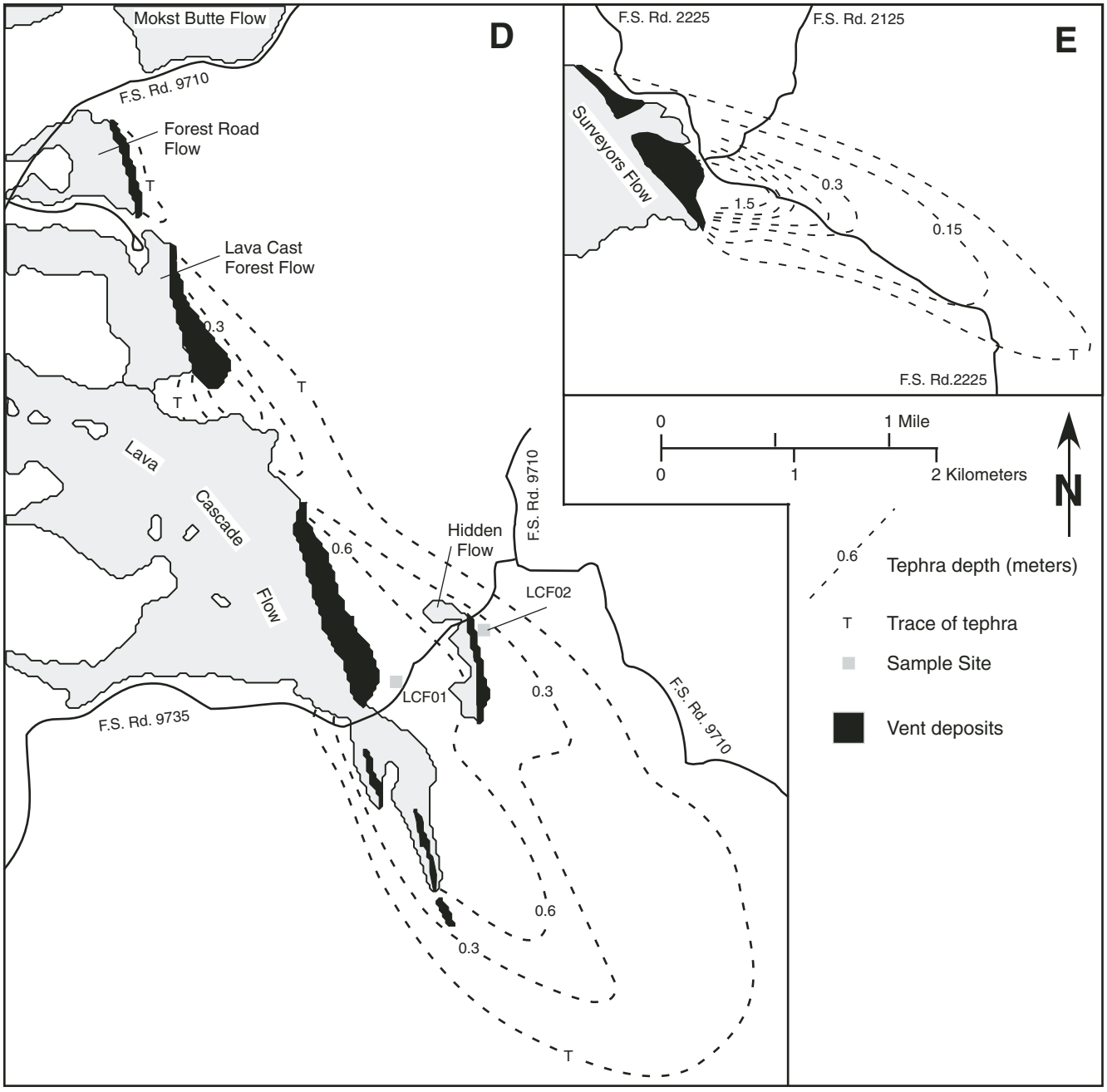

Figure 6 (*continued*).

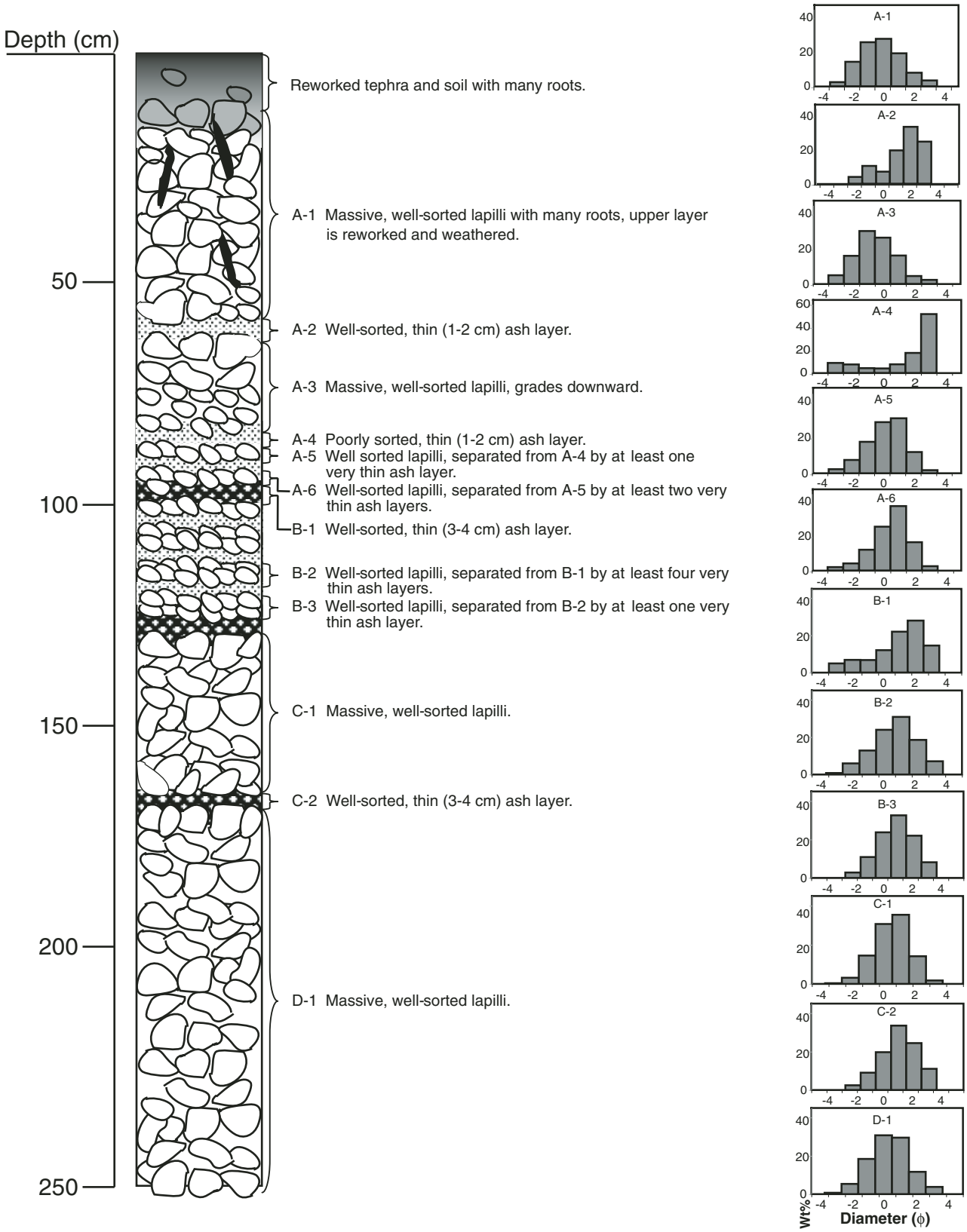

Figure 7. Partial stratigraphic column of the proximal Lava Butte tephra deposit at location LB01, ~300 m northeast of the cone (location shown in Fig. 6A). The sample pit was 2.5 m deep and did not reach the base of the deposit. Four stratigraphic horizons (A–D) were identified based on contacts between massive lapilli layers and distinctive fine ash layers. Each horizon was further subdivided based on changes between fine ash and fine to coarse lapilli. Histograms on the right show grainsize data for samples collected from each horizon. Individual layers are well-sorted and average grainsize is smaller than the Lava Cascade tephra (grainsize data shown in Fig. 12).

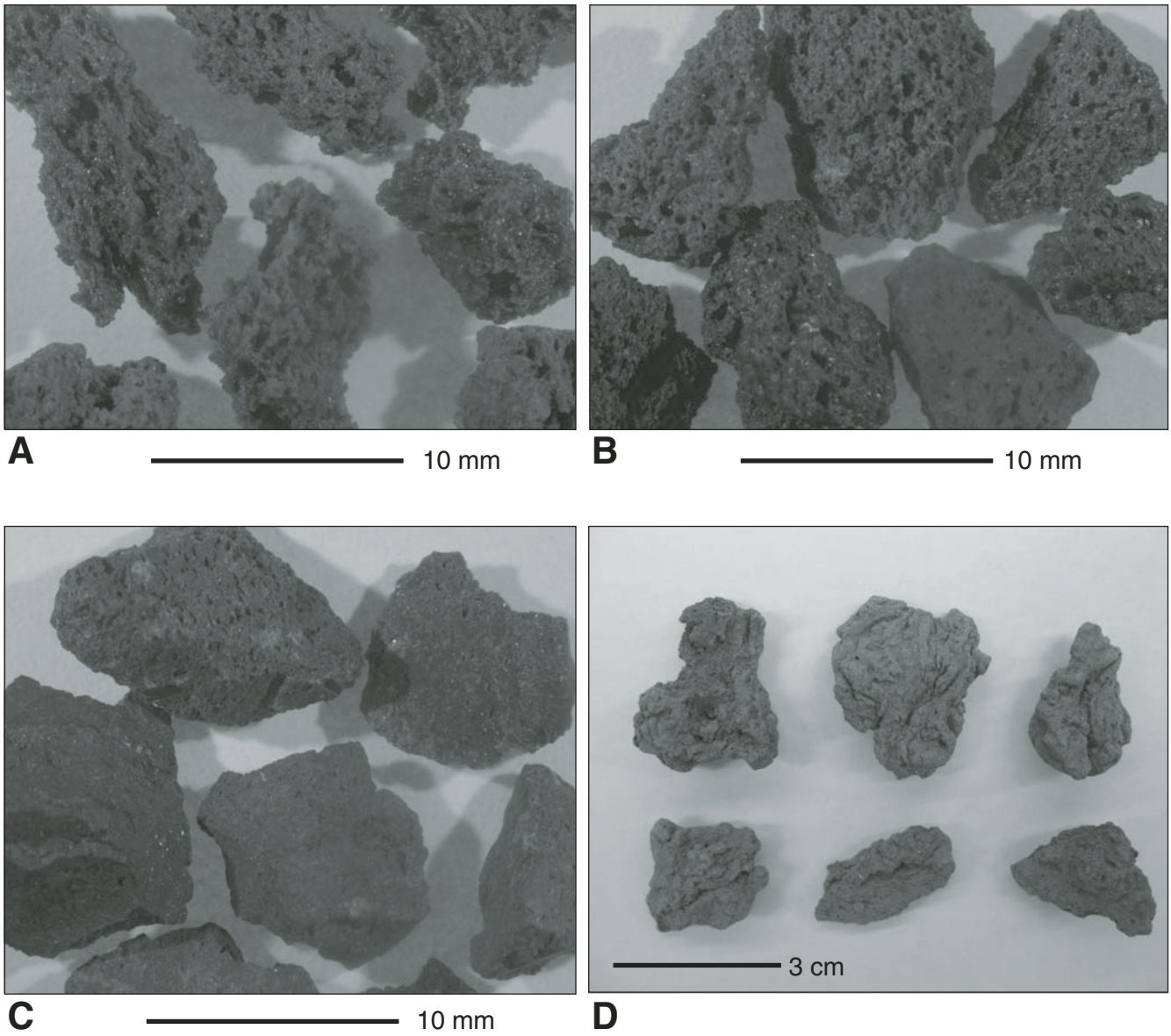

Figure 8. Three components of the Lava Butte tephra: (A) tan, highly vesicular scoria (sideromelane), (B) black, less vesicular scoria (tachylite), and (C) dense fragmented lava. The tephra deposit also contains lapilli pyroclasts that resemble tan scoria but have flattened shapes with relatively smooth wavy surfaces (D).

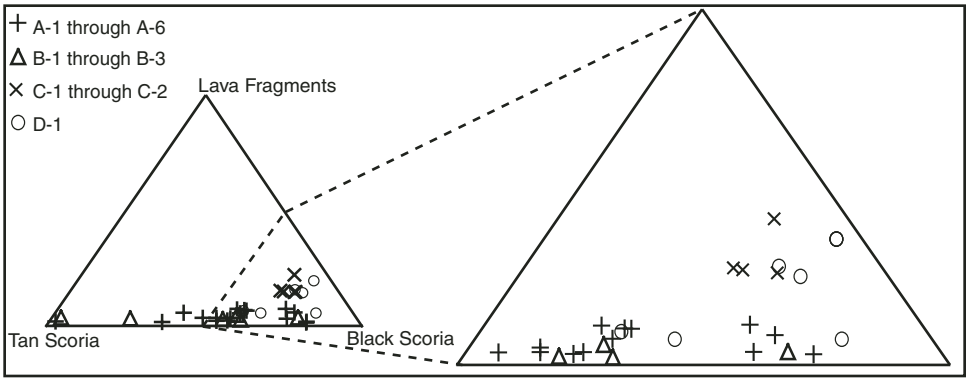

Figure 9. Componentry of stratigraphic horizons A–D of the Lava Butte tephra deposit. Black, less vesicular scoria dominates in horizons deposited during early phases of the eruption (C and D). Proportions of dense fragmented lava are also higher in these horizons. Horizons deposited during later phases of the eruption (A and B) are also dominated by black scoria, but show increasing proportions of tan, highly vesicular scoria.

Activity was concentrated along a segment of the fissure ~1.5 km long and ~250 m wide. Densely welded spatter cones and ramparts up to ~10 m high were formed along this segment of the fissure system. A tephra blanket covering ~8 km^2 was deposited to the southeast. The proximal deposit is >1.5 m thick and present-day trace deposits extend ~4 km from the vents. Total estimated volume of the tephra deposit is ~1.6×10^6 m^3 dense rock equivalent (Table 1), which is probably a minimum. Lava flows extend ~6 km to the west and northwest and cover an area of ~7 km^2.

Samples of the Lava Cascade tephra were collected from two pits located ~250 m (LCF01) and ~850 m (LCF02) from the south end of the main set of vents (Fig. 6D). At LCF01, the deposit is >1.5 m thick (the sample pit did not reach the base of the tephra). This deposit was separated into three stratigraphic horizons based on gradational changes in clast size (Fig. 12). The entire exposed deposit is poorly sorted and average clast diameter increases with depth (Fig. 12). Large clasts are distinctively vesicular and glassy (Fig. 11). In contrast to the three types of clasts in the Lava Butte tephra (Fig. 8), the Lava Cascade tephra is composed of just one component, tan highly vesicular scoria similar to the tan scoria in the Lava Butte deposit.

Interpretation of Eruption Style

Using terminology applied in other volcanic areas around the world, we use the term "Strombolian" to describe the eruptive

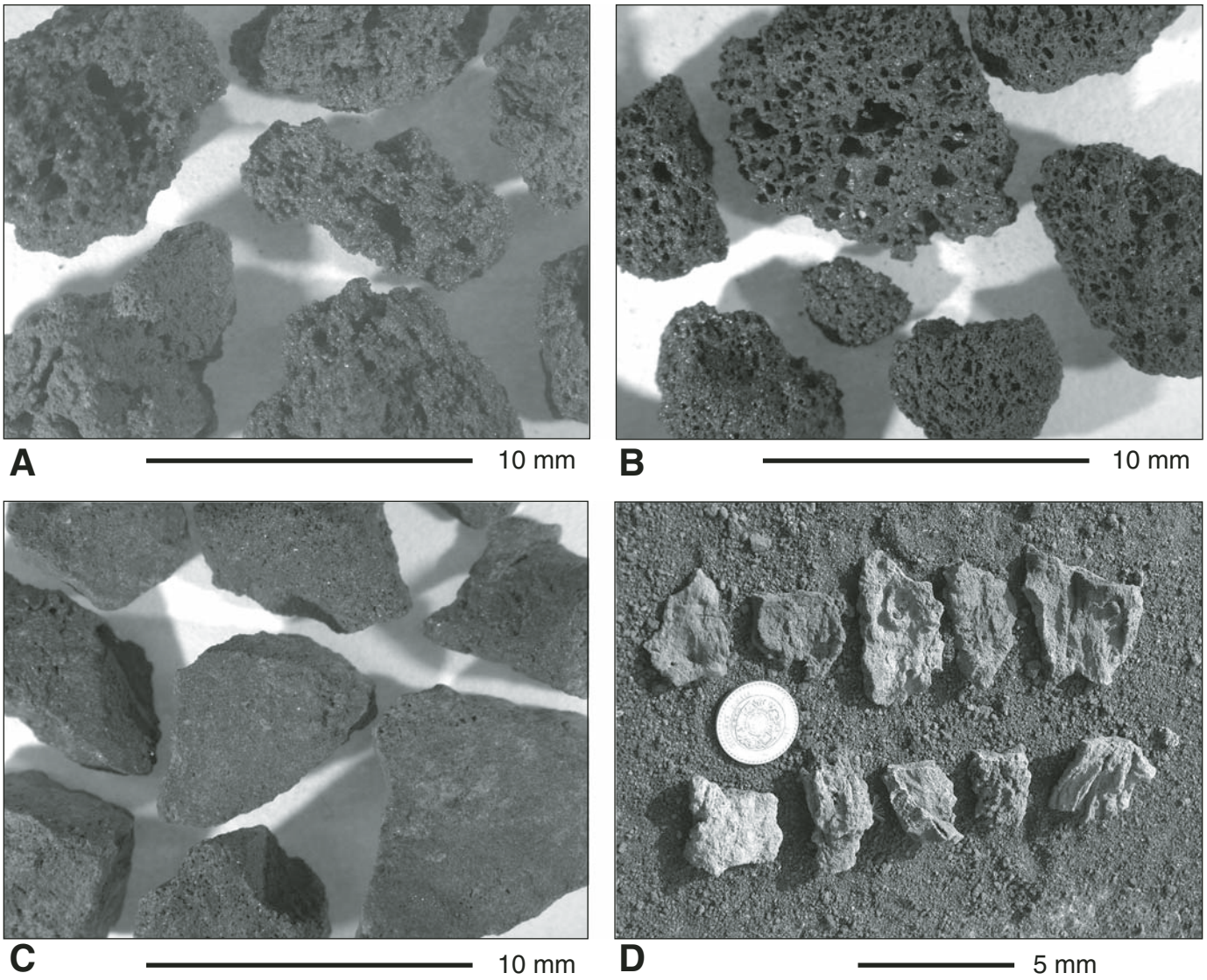

Figure 10. Three components of the tephra from Paricutin, Mexico, as described by Pioli et al., 2008: (A) tan, highly vesicular scoria (sideromelane), (B) black, less vesicular scoria (tachylite), and (C) dense fragmented lava. Flattened clasts with relatively smooth surfaces (D) have also been observed in the tephra deposit from Paricutin (Pioli et al., 2008). Photos A, B, and C courtesy of Kathy Cashman; photo D from Pioli et al. (2008).

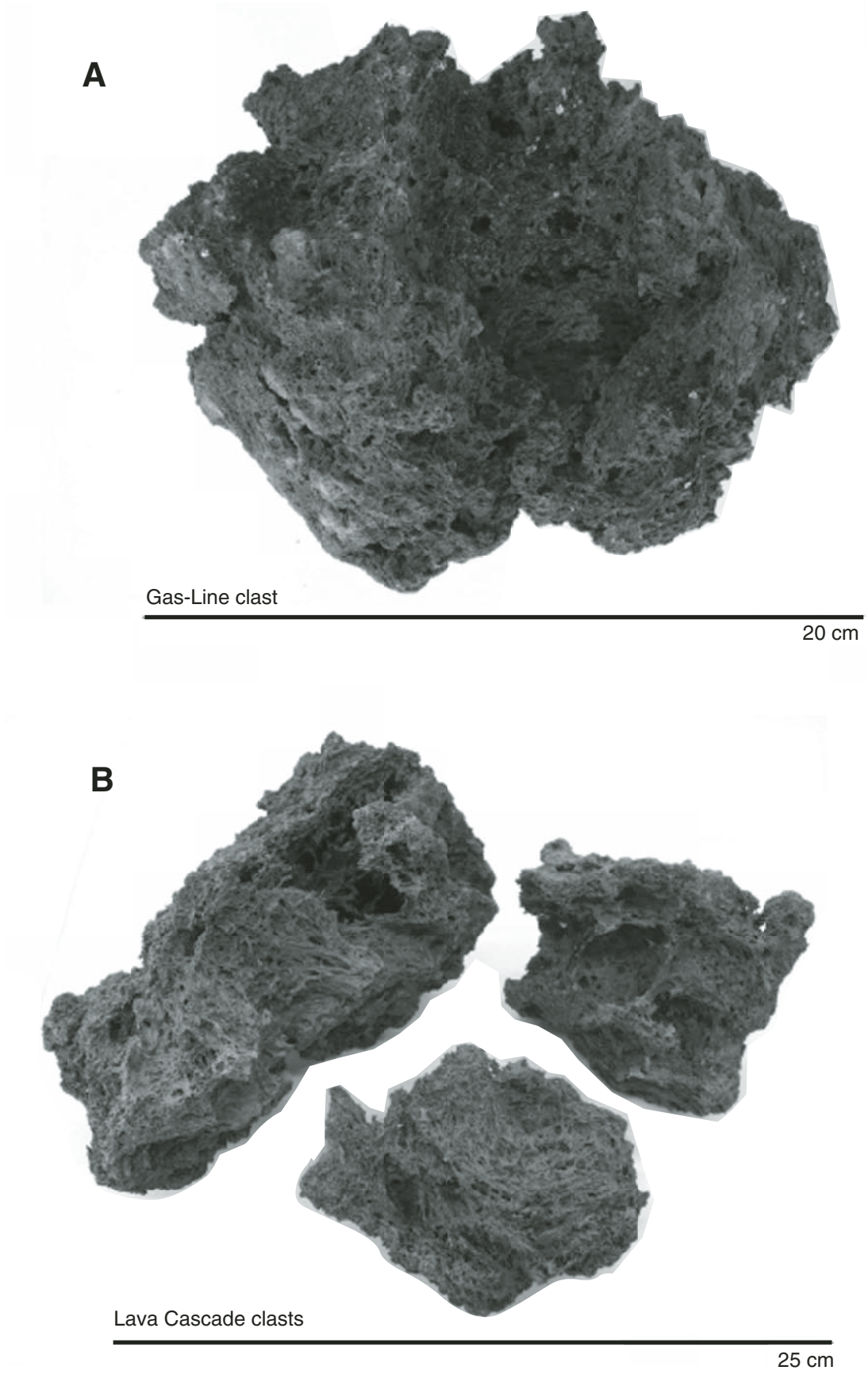

Figure 11. Examples of large, very vesicular glassy clasts common in the Gas-Line and Lava Cascade tephra deposits. These clasts resemble products formed during Hawaiian-style lava fountaining (e.g., Mangan and Cashman, 1996).

style that produced Lava Butte, and "Hawaiian" to describe the style of eruption that produced the Lava Cascade vents. **Hawaiian eruptions** (e.g., Parfitt, 1998; Francis and Oppenheimer, 2004; Valentine and Gregg, 2008) are characterized by effusive fissure eruptions with lava fountains 100s of meters high. These eruptions typically produce spatter ramparts and cones and extensive 'a'a and pahoehoe lava flows. Pyroclastic material is usually limited to proximal deposits and includes coarse lapilli and bombs. Hawaiian-type spatter cones are constructed of moderately to densely welded clasts (Valentine and Gregg, 2008). **Strombolian eruptions** (e.g., Francis and Oppenheimer, 2004; McGetchin et al., 1974; Valentine and Gregg, 2008) are characterized by intermittent, often rhythmic, explosions or fountaining of ballistic pyroclasts and weak eruption columns <1 km high. Cones are constructed at the angle of repose by the ejection of spatter, loose scoria, blocks, and bombs. Extensive 'a'a lava flows are commonly produced, as are fine to coarse tephra deposits that are decimeters to ~1 m thick and localized within 100s of meters from the vent. **Violent Strombolian eruptions** (e.g., Walker, 1973; Arrighi et al., 2001; Valentine and Gregg, 2008; Pioli et al., 2008) have been described as explosive activity that includes ejection of ballistic pyroclasts, voluminous ash production, and sustained eruption columns up to 10 km high. Cinder cones generated by these violent eruptions display internal planar stratification not seen in cones produced by typical Strombolian activity (Valentine and Gregg, 2008). Ash-rich tephra blankets are produced that can be 10s of meters thick near the cone and extend 1 km to 10s of kilometers from the vent. Extensive 'a'a lava flows may also be produced. Pioli et al. (2008) have described violent Strombolian eruptions as being characterized by simultaneous explosive activity from a cinder cone vent and effusive activity from lateral vents.

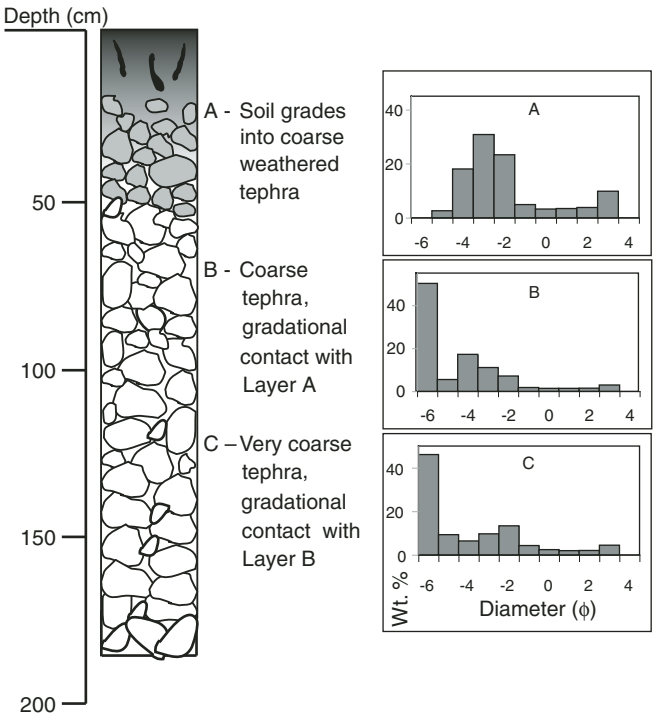

Figure 12. Stratigraphic column of the proximal Lava Cascade tephra deposit at location LCF01, ~250 m south of the vents (location shown in Fig. 6D). The sample pit was 1.5 m deep and did not reach the base of the deposit. Three stratigraphic horizons were identified based on gradational changes in clast size. Histograms on the right show grainsize data for samples collected from each horizon. The deposit is poorly sorted with average grainsize larger than the Lava Butte tephra (compare Fig. 7).

Study of the Lava Butte and Lava Cascade tephra deposits produced during the NWRZ eruption reveals important physical differences between deposits produced by different vents. Preliminary inferences based on the compiled observations of eruption styles listed above are presented here. The Lava Butte tephra deposit is >5 m thick near the vent, and presumably it originally extended >2.5 km from the vent prior to removal of trace deposits through erosional processes. Average grain size is small relative to the Gas-Line and Lava Cascade vents, suggesting the eruption was more explosive. The Gas-Line tephra is less voluminous, is limited to areas proximal to the vents, and contains very large clasts. This suggests that the Lava Butte–Gas-Line fissure eruption began as a Hawaiian-style eruption, but over time became Strombolian to violent Strombolian in style. The Gas-Line vents produced small, welded spatter cones and a limited tephra blanket characterized by massive lapilli layers and large, very vesicular glassy clasts. The Lava Butte vent farther down the fissure (Fig. 6) produced a large cinder cone and a more voluminous tephra blanket characterized by alternating layers of fine ash and lapilli. Physical characteristics of the Lava Butte tephra are similar to tephra characteristics from Paricutin, Mexico, the type example of violent Strombolian activity (e.g., Macdonald, 1972; Walker, 1973). Complex layers of alternating fine ash and lapilli have been interpreted to be the result of hundreds of highly explosive eruptive pulses at Paricutin (Pioli et al., 2008). The Lava Butte tephra deposit is proportionally much smaller than that of Paricutin, but the stratigraphy is similar (Fig. 13). Alternating layers of fine ash and lapilli, though not as complex as the Paricutin stratigraphy, suggest there were at least several phases of highly explosive pulses. Additionally, the three components and the flattened clasts in the Lava Butte tephra are very similar to components identified in tephra from Paricutin (Fig. 10).

The Lava Cascade eruption appears to have been similar to the early phase of the Lava Butte–Gas-Line eruption. Densely welded spatter cones and ramparts were produced along fissure vents and the limited tephra blanket is characterized by massive poorly sorted lapilli layers and large, very vesicular, glassy clasts. Massive lapilli layers suggest that eruption intensities were constant during tephra production, unlike the pulses of highly explosive activity that produced fine ash during the Lava Butte eruption. Large glassy clasts and tephra dominated by one (highly vesicular) component are similar to products formed during Hawaiian-style lava fountaining (e.g., Mangan and Cashman, 1996). Absence of a cinder cone suggests the

Lava Cascade eruption was not characterized by phases of Strombolian activity.

THE NWRZ AND HAZARDS IMPLICATIONS

The potential hazards of mafic eruptions are commonly underappreciated despite the abundance of this type of volcanic activity. Mafic eruptions can continue for days to years, and some vents remain intermittently active for decades to centuries (e.g., Hill et al., 1998). They can produce eruption columns as high as 10 km or more (Arrighi et al., 2001). Tephra production poses hazards to air and ground traffic, property, agricultural production, and human health. In addition to tephra, mafic vents often produce extensive lava flows that can block roads, start forest fires, and alter the flow of surface water.

The city of Bend, Oregon, is located adjacent to the Deschutes River, which was blocked and partially diverted by lava flows from the NWRZ eruption. The blockage of the river would have resulted in at least temporary ponding of water behind the lava dam. If such an event took place today, housing developments upstream would suffer flooding and sudden release of the ponded water would endanger downtown Bend. Large tephra eruptions would also be a serious problem for Bend if winds blew from the south during the eruption. Study of the Lava Butte tephra indicates that at least three pulses of explosive activity took place early in the eruption. During a similar eruption, residents of Bend and nearby communities would likely have to deal with volcanic ash and its accompanying inconvenience, property damage, and possible health impacts. Even a small lava flow that crossed U.S. Highway 97 (Figs. 1 and 2) and the railroad tracks just west of the highway would cause major economic disruption. Multiple lava flows erupted in forested terrain during dry summer months would undoubtedly result in forest fires with their attendant hazards.

Eruptions like the NWRZ that produce multiple vents and lava flows may persist intermittently for years or even decades. New geologic mapping and paleomagnetic work indicate that multi-vent, multi-flow eruptions are common at Newberry Volcano. The opening of a single vent would not preclude additional vents opening over an extended area. Understanding the nature

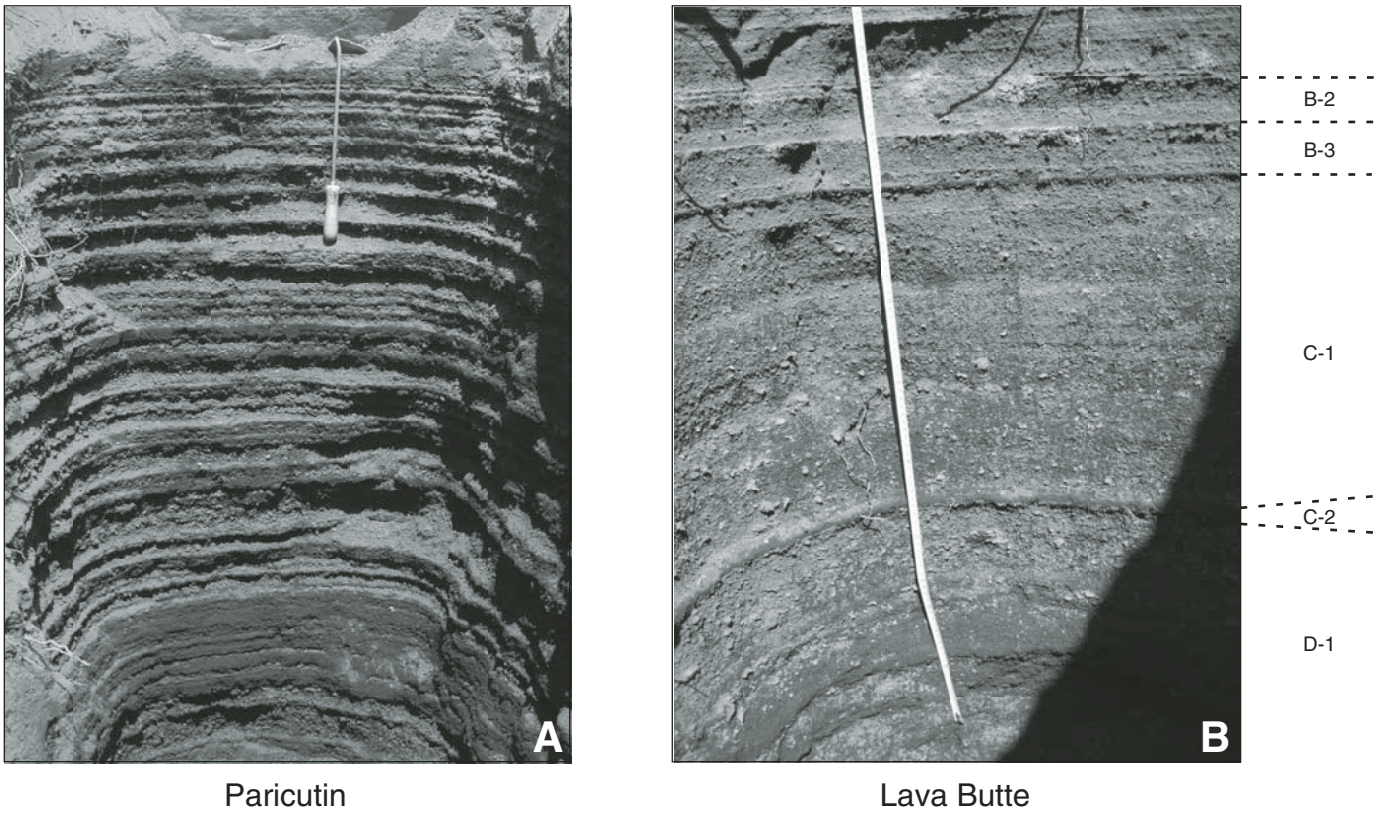

Figure 13. Photographs of Lava Butte and Paricutin, Mexico, tephra deposits. (A) The Paricutin deposit shows finely stratified layers of alternating fine ash and lapilli, which has been interpreted as the result of hundreds of highly explosive eruptive pulses (Pioli et al., 2008). Approximate visible section of depth is 1.1 m. (B) The Lava Butte deposit also shows alternating layers of fine ash and lapilli, although not as finely stratified as at Paricutin. Alternating layers in stratigraphic horizon B suggest there were at least several phases of highly explosive activity during the Lava Butte eruption. Approximate visible section of depth is 1 m. For complete stratigraphic column see Figure 7. (Paricutin photo courtesy of Kathy Cashman).

and duration of this eruption will provide context for any future similar events.

CONCLUSIONS AND SUGGESTIONS FOR FUTURE WORK

The NWRZ eruption is the youngest mafic eruption at Newberry Volcano. It took place ~7000 years ago, subsequent to deposition of the Mazama ash. Multiple vents produced lava flows over a distance of 32 km from the Deschutes River on the northwest to East Lake in Newberry caldera, and farther south to the upper southwest flank of Newberry Volcano. Eruptive activity may have been episodic and could have continued intermittently for many decades. Erupted compositions range from basalt to andesite. At least one large cinder cone, Lava Butte, produced tephra plumes that likely would have reached the city of Bend when winds were blowing from the south. Previous data and interpretations about the NWRZ were reassessed. Two lava flows previously assigned to the eruption were excluded based on stratigraphy and geochemistry.

Lava flows from the NWRZ eruption crossed the present locations of busy U.S. Highway 97 and the adjacent railroad tracks, and blocked the Deschutes River, causing it to partially change its course. Another such eruption would likely endanger downtown Bend as well as upstream communities from potential flooding and volcanic ashfall, in addition to possible blockage of major transportation corridors and damage to utility corridors, resulting in significant economic consequences.

Among suggestions for new work on the NWRZ, we list first a petrologic study. No petrologic work has been done on the NWRZ. Also, better age control could perhaps be obtained by careful sampling of additional large tree molds that exist in some of the more fluid lava flows, or by finding small charcoal fragments such as burned pine needles under the tephra deposits. Additional paleomagnetic sampling would help to constrain the possible time span of eruptive activity.

ACKNOWLEDGMENTS

We are grateful to M. Clynne and M. Patrick for their thorough and very helpful reviews.

REFERENCES CITED

Arrighi, S., Principe, C., and Rosi, M., 2001, Violent strombolian and subplinian eruptions at Vesuvius during post-1631 activity: Bulletin of Volcanology, v. 63, p. 126–150, doi: 10.1007/s004450100130.

Champion, D.E., 1980, Holocene geomagnetic secular variation in the western United States: Implications for the global geomagnetic field: U.S. Geological Survey Open File Report 80-824, 314 p.

Champion, D.E., and Shoemaker, E.M., 1977, Paleomagnetic evidence for episodic volcanism on the Snake River Plain: Planetary Geology Field Conference on the Snake River Plain, Idaho, October 1977: NASA Technical Memorandum 78436, p. 7–8.

Francis, P., and Oppenheimer, C., 2004, Volcanoes: Oxford University Press, New York, 135 p.

Hagstrum, J.T., and Champion, D.E., 2002, A Holocene paleosecular variation record from ^{14}C-dated volcanic rocks in western United States: Journal of Geophysical Research, v. 107, 14 p.

Hallett, D.J., Hills, L.V., and Clague, J.J., 1997, New accelerator mass spectrometry radiocarbon ages for the Mazama tephra layer from Kootenay National Park, British Columbia, Canada: Canadian Journal of Earth Sciences, v. 34, p. 1202–1209, doi: 10.1139/e17-096.

Heiken, G., 1978, Characteristics of tephra from Cinder Cone, Lassen Volcanic National Park, California: Bulletin of Volcanology, v. 41–2, p. 119–130.

Hill, B.E., Connor, C.B., Jarzemba, M.S., LaFemina, P.C., Navarro, M., and Strauch, W., 1998, 1995 eruptions of Cerro Negro volcano, Nicaragua, and risk assessment for future eruptions: Geological Society of America Bulletin, v. 110, no. 10, p. 1231–1241, doi: 10.1130/0016-7606(1998)110<1231:EOCNVN>2.3.CO;2.

Jensen, R.A., 2006, Roadside guide to the geology and history of Newberry Volcano, 4th Ed.: Bend, Oregon, CenOreGeoPub, 182 p.

Jensen, R.A., Donnelly-Nolan, J.M., and Mckay, D.M., 2009, A field guide to Newberry Volcano, Oregon, *in* O'Connor, J.E., Dorsey, R.J., and Madin, I.P., eds., Volcanoes to Vineyards: Geologic Field Trips through the Dynamic Landscape of the Pacific Northwest: Geological Society of America Field Guide 15, doi: 10.1130/2009.fld015(03).

MacLeod, N.S., and Sherrod, D.R., 1988, Geologic evidence for a magma chamber beneath Newberry volcano, Oregon: Journal of Geophysical Research, v. 93, no. B9, p. 10067–10079, doi: 10.1029/JB093iB09p10067.

MacLeod, N.S., Sherrod, D.R., Chitwood, L.A., and Jensen, R.A., 1995, Geologic Map of Newberry volcano, Deschutes, Klamath, and Lake Counties, Oregon: U.S. Geological Survey Miscellaneous Geologic Investigations Map I-2455, scale 1:62,500.

Macdonald, G.A., 1972, Volcanoes: Prentice-Hall Inc., Englewood Cliffs, New Jersey, 510 p.

Mangan, M.T., and Cashman, K.V., 1996, The structure of basaltic scoria and reticulite and inferences for vesiculation, foam formation, and fragmentation in lava fountains: Journal of Volcanology and Geothermal Research, v. 73, no. 1–2, p. 1–18, doi: 10.1016/0377-0273(96)00018-2.

McGetchin, T.R., Settle, M., and Chouet, B.A., 1974, Cinder cone growth modeled after Northeast crater, Mount Etna, Sicily: Journal of Geophysical Research, v. 79, no. 23, p. 3257–3272, doi: 10.1029/JB079i023p03257.

McKnight, S.B., and Williams, S.N., 1997, Old cinder cone or young composite volcano?: The nature of Cerro Negro, Nicaragua: Geology, v. 25, no. 4, p. 339–342, doi: 10.1130/0091-7613(1997)025<0339:OCCOYC>2.3.CO;2.

Miyashiro, A., 1974, Volcanic rock series in island arcs and active continental margins: American Journal of Science, v. 274, p. 321–355.

Nichols, R.L., and Stearns, C.E., 1938, Fissure eruptions near Bend, Oregon [abs.]: Geological Society of America Bulletin, v. 49, no. 12, pt. 2, p. 1894.

Parfitt, E.A., 1998, A study of clast size distribution, ash deposition and fragmentation in Hawaiian-style volcanic eruptions: Journal of Volcanology and Geothermal Research, v. 84, p. 197–208, doi: 10.1016/S0377-0273(98)00042-0.

Peterson, N.V., and Groh, E.A., eds., 1965, Lunar Geological Field Conference Guide Book: Oregon Department of Geology and Mineral Industries Bulletin, 51 p.

Pioli, L., Erlund, E., Johnson, E., Cashman, K., Wallace, P., Rosi, M., and Delgado Granados, H., 2008, Explosive dynamics of violent Strombolian eruptions: The eruption of Paricutin Volcano 1943–1952 (Mexico): Earth and Planetary Science Letters, v. 271, p. 359–368.

Valentine, G.A., and Gregg, T.K.P., 2008, Continental basaltic volcanoes—Processes and problems: Journal of Volcanology and Geothermal Research, v. 177, p. 857–873, doi: 10.1016/j.jvolgeores.2008.01.050.

Walker, G.P.L., 1973, Explosive volcanic eruptions—A new classification scheme: Geologische Rundschau, v. 62, p. 431–446, doi: 10.1007/BF01840108.

Williams, H., 1935, Newberry volcano of central Oregon: Geological Society of America Bulletin, v. 46, no. 2, p. 253–304.

Manuscript Accepted by the Society 18 June 2009